INSTITUTE OF PHYSICS PUBLISHING NANOTECHNOLOGY
Nanotechnology **17** (2006) 283–288 doi:10.1088/0957-4484/17/1/048

One-step synthesis of 3D dendritic gold/polypyrrole nanocomposites via a self-assembly method

Kun Huang, Yuanjian Zhang, Dongxue Han, Yanfei Shen, Zhijuan Wang, Junhua Yuan, Qixian Zhang and Li Niu[1]

State Key Laboratory of Electroanalytical Chemistry, Changchun Institute of Applied Chemistry, Graduate School of the Chinese Academy of Sciences, Chinese Academy of Sciences, Changchun 130022, People's Republic of China

E-mail: lniu@ciac.jl.cn

Received 26 July 2005, in final form 29 September 2005
Published 5 December 2005
Online at stacks.iop.org/Nano/17/283

Abstract
Novel spherical three-dimensional (3D) dendritic gold–polypyrrole nanocomposites were successfully prepared in the presence of an amphiphilic *p*-toluene sulfonic acid (TSA) as dopant and surfactant via a self-assembly process which is based on the oxidation of pyrrole (Py) and the reduction of the chloroaurate ions, yielding PPy and Au(0) simultaneously. It was found that the probability of obtaining dendritic Au@PPy/TSA nanostructures depended on the concentration of TSA and the rate of addition of the oxidant ($HAuCl_4$). It was also proposed that the supramolecular micelles formed by Py and TSA play the role of a 'soft template' to produce the dendritic Au@PPy/TSA nanocomposites.

1. Introduction

Nanocomposites of conducting polymers and metal nanoparticles have received considerable attention due to the potential possibilities to create suitable materials for electrocatalysis, chemical sensors, and microelectronic devices [1–3]. Conducting polymers are well known for their excellent electronic properties with conductivity covering the whole range from insulator to metal while retaining the light-weight, mechanical properties and processing advantages of polymers [4]. Compared with nanocomposites constructed by insulating polymers, conducting polymers can serve as a novel electroactive relay among these metal nanoparticles in the nanocomposites matrix [5, 6]. For example, it has been reported that conducting polymer-supported platinum and rhodium catalysts show potential applications to novel catalysts because the conducting polymers might shuttle the electronic charge to catalyst centres [7, 8]. On the other hand, metal nanoparticles incorporated into conducting polymers are also known to enhance the conductivity of the polymers [9, 10]. Therefore, the fabrication of novel nanocomposites based upon metal nanoparticles and conducting polymers would provide various interesting characteristics and new features in nano-technological applications.

Among these reported metal clusters, gold nanoparticles as well as nanorods have attracted much attention owing to their unique optical, electrical and photocatalytic properties depending on their sizes and shapes [11–13]. Recently, a variety of methods have been explored to achieve gold nanoparticle–conducting polymer composites. Overall, three different approaches have been used to date. The first one is the electrochemical method, which is based on the oxidation of the individual monomer and further incorporation of the metallic species deposited from an aqueous solution containing a suitable cation [14, 15]. The second technique consists of *in situ* preparation of the gold nanoparticles in the polymer matrix, which might open up much wider possibilities for the gold-conducting polymer applications. By this method, Hatchett and Chattopadhyay have reported the chemical synthesis of a polyaniline/gold composite using tetrachloroaurate [16, 17]. Liu has also demonstrated that the polypyrrole-stabilized gold nanostructures can be formed on roughened gold substrates through a similar reaction based on gold ions and pyrrole [18, 19]. In particular,

[1] Author to whom any correspondence should be addressed.

Selvan and co-workers have shown that the reduction of $AuCl_4^-$ ions sequestered in micelles of a diblock copolymer results in the formation of gold nanoparticles capped into polypyrrole bulk matrix [20]. In addition, they have also observed the Au–PPy dendritic nanostructures employing vapour phase polymerization of pyrrole onto a solution-cast film of block copolymer ionomers [21]. The third technique involves the synthesis of Au nanoparticles, and coating the Au nanoparticles on PPy templates [22] or polymerization of Py using the Au nanoparticles as a template [23]. In the above-mentioned works, much emphasis was focused on the structure and properties of gold-conducting polymer composite; however, there are very few reports addressed to the fabrication of unusual dendritic gold nanostructures in a matrix of polypyrrole [21] by a simple liquid phase reaction.

Herein, a novel method is reported to synthesize 3D dendritic gold/polypyrrole (Au@PPy/TSA) nanocomposites via a self-assembly process in which pyrrole monomer is oxidized by chlorauric acid ($HAuCl_4$) in the presence of TSA. In this preparation, the hydrophilic $–SO_3H$ group of TSA functionalizes as a dopant and a surfactant at the same time. The dopant role resulted in the improvement of electrical properties of the polypyrrole layer, and the surfactant role acted as a soft template in the formation of 3D nanodendritic structure.

2. Experimental section

16.7 μl of distilled pyrrole monomer was mixed with 25 ml TSA aqueous solution (0.1 M) under stirring for 0.5 h to obtain a uniform emulsion. 5 ml of aqueous solution of $HAuCl_4$ (5 mM) was added to the emulsion. The mixture was allowed to react at 0–5 °C (in an ice bath) for 10 h under stirring. Then, the product was washed with de-ionized water, methanol, and ethyl ether several times, dried under vacuum for 24 h, and finally a dark power of Au@PPy/TSA nanocomposites was obtained. The synthetic route of Au@PPy/TSA composites is illustrated as follows:

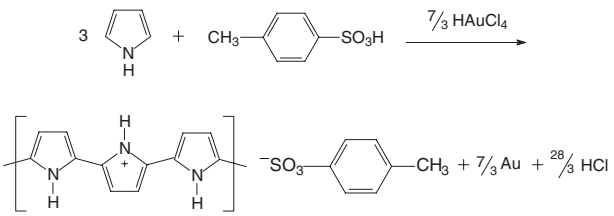

The morphology of Au@PPy/TSA nanocomposites was proved by scanning electron microscope (SEM, XL30 ESEM FEG) and transmission electron microscope (TEM, JEOL2000). Ultraviolet–visible (UV–vis) absorption spectra of Au@PPy/TSA nanocomposites dispersed in aqueous solution were recorded on a UV-3100 spectrometer. FTIR (Perkin-Elmer system) and x-ray diffraction (MAC Science, Japan M-18AHF) measurements were performed to characterize the structure of Au@PPy/TSA nanocomposites.

3. Results and discussion

Figure 1 shows typical SEM images of such 3D dendritic Au@PPy/TSA nanocomposites. The Au@PPy/TSA

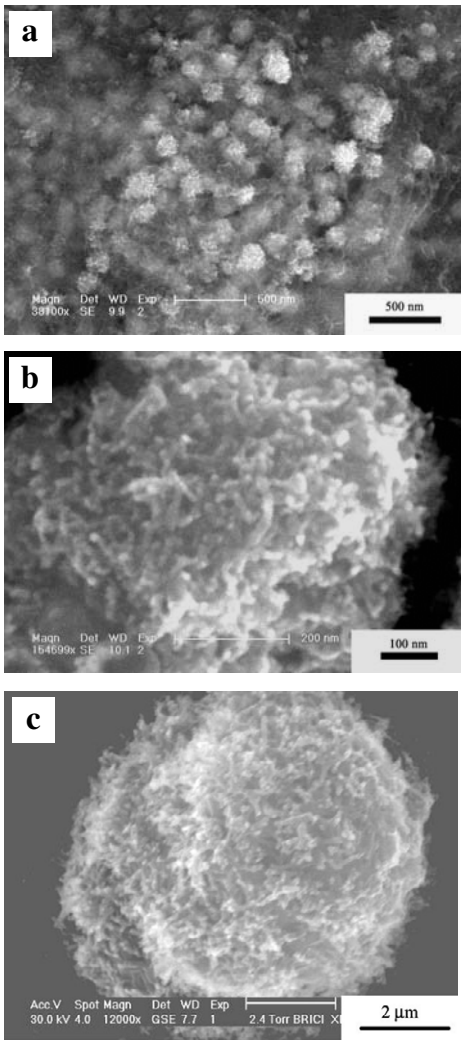

Figure 1. SEM images of the 3D dendritic Au@PPy/TSA nanocomposites and the surface of a natural lotus leaf: (a) at low magnification; (b) an enlarged view of an individual sphere shown in (a); (c) surface microstructure of the natural lotus leaf.

nanocomposites show evident spherical morphology (yield >90%), as seen in figure 1(a), and these spherical Au@PPy/TSA nanocomposites are well dispersed in amorphous colloidal polypyrrole matrix. Electron micrographs of an individual spherical Au@PPy/TSA nanocomposite at higher magnification were shown in figure 1(b). Interestingly, on the surface of nanoscale spherical Au@PPy/TSA composites, many dendritic Au@PPy/TSA nanorods can be observed. In particular, the surface of spherical Au@PPy/TSA nanocomposites shows a bionic nano-nanoscale binary structure, similar to the natural lotus leaf, where every microscale papilla on the leaf surface is covered by nanoscale papillae (figure 1(c)) [24].

The 3D dendritic structure of spherical Au@PPy/TSA nanocomposites is more clearly seen in figures 2(a) and (b). The average diameter of the spherical Au@PPy/TSA nanocomposites was estimated to be ca 80–150 nm, and they were rather polydisperse. The detailed structure of the 3D dendritic Au@PPy/TSA nanocomposites is further revealed by high-resolution TEM images and an electron diffractogram. Figure 2(b) shows the sphere structure at higher

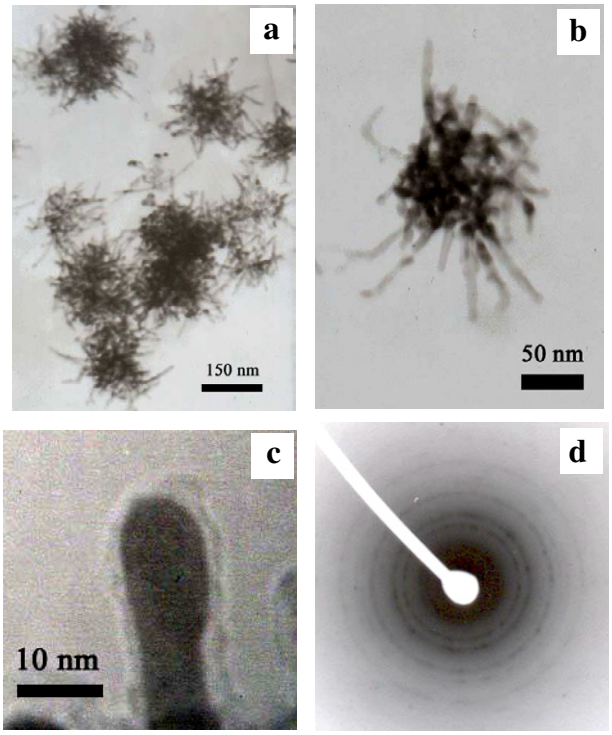

Figure 2. Typical TEM images of the 3D dendritic Au@PPy/TSA nanocomposites: (a) at low magnification; (b) at high magnification; (c) a magnification view of an individual Au@PPy/TSA nanorod arm in dendrites. (d) Transmission TEM diffraction image (reaction conditions: [TSA] = 0.1 M [Py] = 0.1 M, [$HAuCl_4$] = 1.67 M, reaction time = 10 h, temp. = 0–5 °C).

magnification. It can be obviously seen that these spherical Au@PPy/TSA nanocomposites show a 3D dendritic structure and are composed of some fractal-shaped Au@PPy/TSA nanorod arms with an average diameter of ca 8–12 nm and a high aspect ratio (ca 5–10). Moreover, figure 2(c) indicates that the dark Au nanorod arms are surrounded by a greyish amorphous sheath-protected PPy [20, 21]. The electron diffraction pattern of the dendritic Au@PPy/TSA nanocomposites is shown in figure 2(d). Two conclusions can be drawn: firstly, polypyrrole is amorphous, which results in the characteristic rings in the diffraction pattern. Secondly, the diffraction pattern of Au clusters is in the form of spots superimposed on the rings, which is originated from many different crystallographic orientations.

Moreover, it was necessary to understand the mechanism by which the nanodendrites were formed. In this work, it was found that the concentration of dopant TSA and the rate of addition of the oxidant ($HAuCl_4$) strongly affected the morphology of the obtained Au@PPy/TSA nanocomposites. Figure 3 shows a typical example of the effect of the TSA concentration on the morphology measured by TEM. When the TSA concentration was high (1 M), the spherical dendritic aggregates could be observed, as shown in figures 3(a) and (b). Interestingly, highly dispersed regular 3D dendritic morphology with a high aspect ratio could be obtained when the TSA concentration decreased to 0.1 M (figures 3(c) and (d)). However, irregular dendritic-like grain morphology was observed when the TSA concentration further decreased to 0.01 M (figures 3(e) and (f)). Furthermore, in the absence of TSA dopant, the Au agglomeration phenomenon occurred (figures 3(g) and (h)). These results indicate that a change in morphology from dendritic aggregates, to 3D dendrites, to dendritic-like grains, and to agglomerations, took place when the concentration of TSA changed from 1 to 0.1 M, to 0.01 M, and to 0 M, respectively. As described in previous reports [25, 26], the self-assembled micelles play a 'soft-template' role in the formation of the nanostructured PPy. Here, TSA can act as dopant and surfactant at the same time due to the ionized $–SO_3H$ group and the amphiphilicity of TSA. In addition, pyrrole monomer in TSA aqueous solution easily forms Py/TSA micelles by hydrophobic interaction, while addition of an oxidant ($HAuCl_4$), the nucleation and growth of Au, and polymerization of pyrrole take place simultaneously at the water/micelle interface due to the hydrophilicity of this $AuCl_4^-$. As the reaction continues, a 3D dendritic Au@PPy/TSA nanocomposite with high aspect ratio is obtained. It can be proposed that such Py/TSA supramolecular micelles might serve as a 'soft template' and kinetically control the growth rates of various faces of Au nanoparticles by selectively adsorbing onto the crystallographic planes, thus resulting in the dendritic morphology. The results also suggest that such Py/TSA 'soft-template' supramolecular micelles might be destroyed when the concentration of TSA increases or decreases, and thus the morphology of the obtained Au@PPy/TSA composite changes, which is in agreement with our results (as shown in figures 2(a) and (d)).

In this synthesis, the reduction of pyrrole monomer and the oxidation of the chloroaurate ions ($AuCl_4^-$) occur simultaneously, yielding PPy and zero-valent Au. The polymerization rate of the pyrrole monomer was affected by the polymerization temperature, rate of addition of the oxidant, concentration of the oxidant, and so forth. Here, only the rate of addition of the oxidant is changed to further investigate the influence of the polymerization rate on the morphology of Au@PPy/TSA composites. Figure 4 represents the influence on the rate of addition of the oxidant on the resulting composite morphology. Spherical granular Au@PPy/TSA nanocomposite was obtained when the addition was very quick, ca 1 ml s^{-1} (figures 4(a) and (b)). On the other hand, 3D dendritic Au@PPy/TSA nanocomposites were prepared when the addition was slow, ca 0.1 ml s^{-1}. However, the aspect ratio of the obtained Au@PPy/TSA nanorod arms is low (ca 2–4) (figures 4(c) and (d)). Only when the addition was very slow (0.01 ml s^{-1}) could the regular 3D dendritic Au@PPy/TSA nanocomposites with the high aspect ratio of the fractal-shaped nanorod arms (5–10) be obtained (figures 2(a) and (b)). This indicates that when the polymerization rate was quick, too much PPy–TSA and Au was produced in a very short time, and PPy–TSA and Au did not have enough time to form the regular dendritic morphology via self-assembly; in contrast, when the rate was slow, they easily formed the regular 3D dendritic Au@PPy/TSA nanocomposites through a self-assembly process. The results confirm that the formation of 3D dendritic Au@PPy/TSA nanocomposites described in this study is a slow self-assembly process.

The dark dendritic Au@PPy/TSA nanocomposites could be readily dispersed into water to form a clear and dark suspension, which was quite stable even for several more

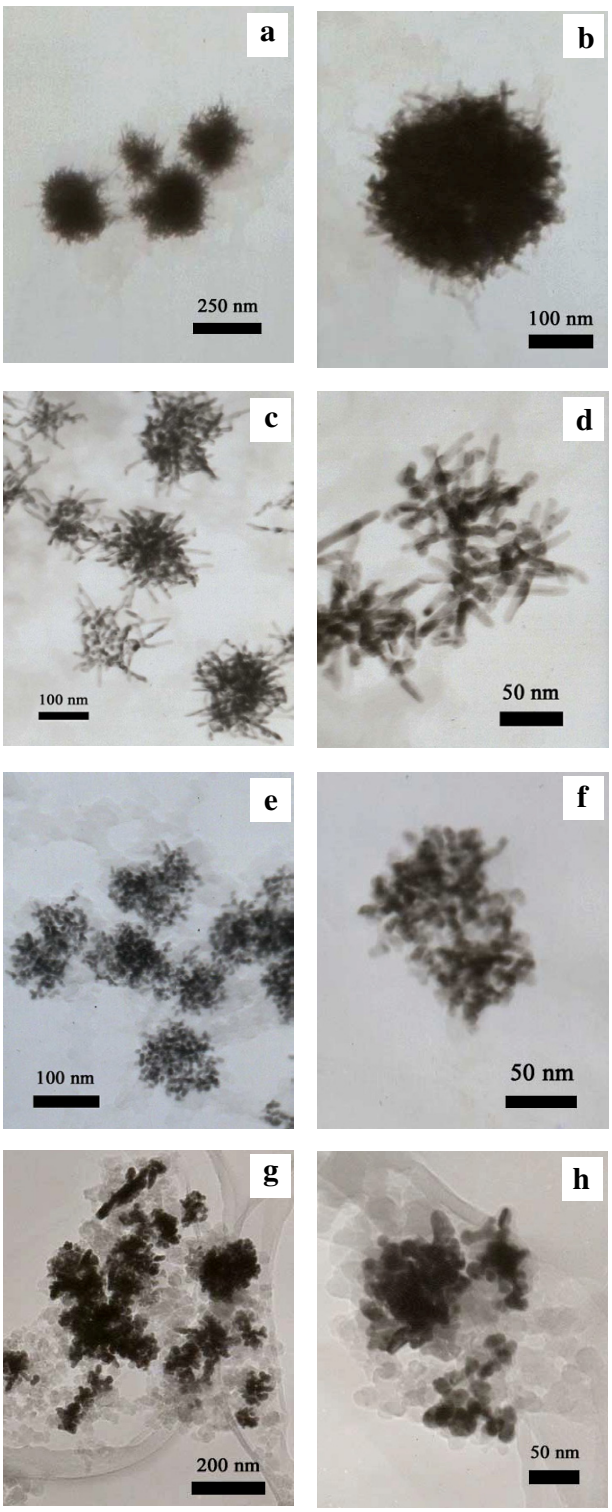

Figure 3. Influence of the concentration of TSA on the morphology of Au@PPy/TSA nanocomposites: ((a), (b)) 1 M; ((c), (d)) 0.1 M; ((e), (f)) 0.01 M; ((g), (h)) 0 M (other reaction conditions: [Py] = 0.1 M, [$HAuCl_4$] = 1.67 M, reaction time = 10 h, temp. = 0–5 °C).

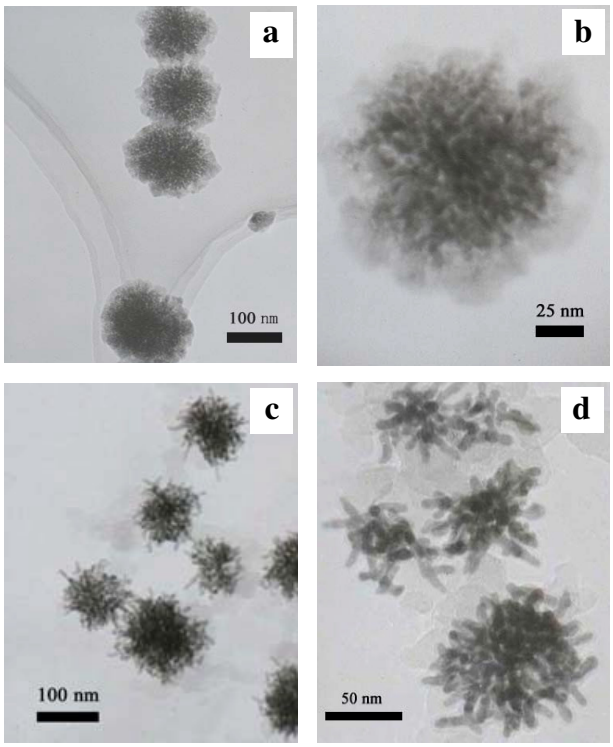

Figure 4. Influence of polymerization rate on the morphology of Au@PPy/TSA nanocomposites synthesized by the self-assembly method: ((a), (b)) very quick and ((c), (d)) slow (other reaction conditions: [TSA] = 0.1 M [Py] = 0.1 M, [$HAuCl_4$] = 1.67 M, reaction time = 10 h, temp. = 0–5 °C).

days. The UV–vis absorption spectrum of the Au@PPy/TSA nanocomposites dispersed in aqueous medium is shown in figure 5. Two typical absorption peaks can be observed at ca 440 and 800 nm, which corresponds to the π–π^* transition of the PPy chain and to a polaron transition similar to that of an ordinary PPy [27]. The absence of the typical surface plasmon resonance of Au(0) around 520 nm for Au/PPy nanocomposites reveals that Au is dispersed as ultra-small clusters of elementary gold within the Au/PPy nanocomposites. This type of Au is characterized by a weak and broad absorption maximum at about 440 nm. But it should be noted that the π–π^* transition of the PPy chain at 400–500 nm overlaps this region. This is consistent with the idea that elementary Au is formed concurrently with PPy. A similar observation was also reported by Liu *et al* [19] and Selvan *et al* [20, 21].

The molecular structure of Au@PPy/TSA nanocomposites was characterized by FTIR spectroscopy (data not shown here) and XRD (in figure 6). In FTIR results, the characteristic bands of polypyrrole, the pyrrole ring fundamental vibrations centred at 1541 and 1448 cm^{-1}, the =C–H in-plane vibrations at 1303, 1161, and 1037 cm^{-1}, and N–H stretching vibration at 3432 cm^{-1}, can be observed well in the Au@PPy/TSA nanocomposites. These results indicate that the structure of the polypyrrole backbone in Au@PPy/TSA nanocomposites is similar to that of conventional PPy synthesized by the well established method [28].

The presence of Au in the Au@PPy/TSA nanocomposites was further confirmed by powder XRD measurements, as shown in figure 6. In the XRD curve of the Au@PPy/TSA nanocomposites, a broad peak centred at $2\theta = 23.3°$ related to the amorphous PPy was observed, which is similar to the

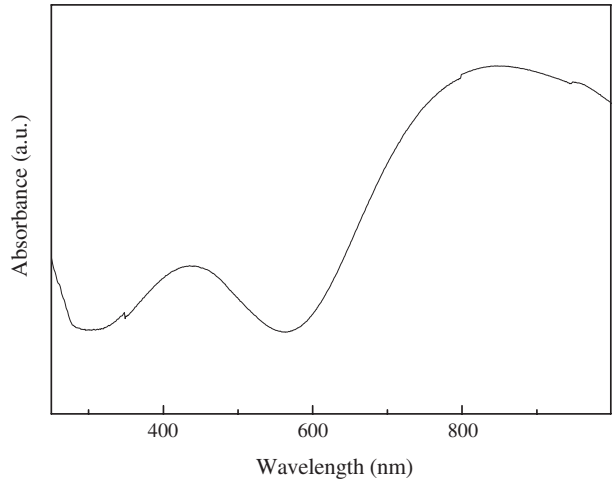

Figure 5. UV–vis spectrum of the dendritic Au@PPy/TSA nanocomposites dispersed in aqueous solution.

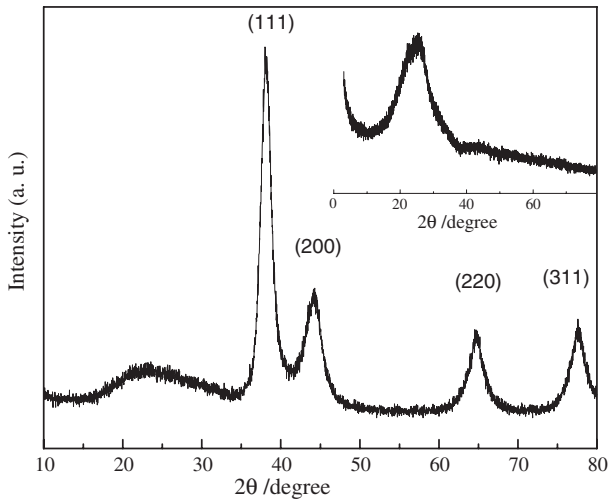

Figure 6. XRD pattern of the dendritic Au@PPy/TSA nanocomposites. The inset shows the XRD pattern of the PPy/TSA alone.

conventional PPy (as shown in the inset in figure 6) [29]. Moreover, four strong bands appeared with maximum intensity at 38.1°, 44.2°, 64.6° and 77.7° representing Bragg's reflections from (111), (200), (220) and (311) planes of Au. The unit cell constant a of such an fcc lattice can be obtained as 4.086 Å, which means that the Au nanodendrites had grown well along all planes.

In conclusion, a simple and novel method has been introduced to prepare 3D dendritic Au@PPy/TSA nanocomposites using $HAuCl_4$ as an oxidant, and TSA as dopant and surfactant. A model of a supramolecular micelle 'soft template' based on pyrrole and TSA is proposed to interpret the formation mechanism of 3D dendritic Au@PPy/TSA nanocomposites. In particular, the synthesized Au@PPy/TSA nanocomposites show a bionic nano-nanoscale binary structure similar to the natural lotus leaf. Furthermore, the method described in this study provides a simple and inexpensive route to prepare inorganic–organic supermolecular nanocomposites.

Acknowledgments

The authors are most grateful to the NSFC, China (No 20475053) and Department of Science and Technology of Jilin Province (No 20050102) for financial support. The authors gratefully acknowledge financial support for the joint projects from NSFC, China (No 20211130506 and No 20320120169) and also from the Academy of Finland.

References

[1] Segawa H, Shimidzu T and Honda K 1989 A novel photo-sensitized polymerization of pyrrole *J. Chem. Soc. Chem. Commun.* 132
[2] Sargent A, Loi T, Gal S and Sadik O A 1999 The electrochemistry of antibody-modified conducting polymer electrodes *J. Electroanal. Chem.* **470** 144
[3] Kern J M and Sauvage J P 1989 Photochemical deposition of electrically conducting polypyrrole *J. Chem. Soc. Chem. Commun.* 657
[4] Skotheim T A, Elsenbaumer R L and Reyholds J F 1998 *Handbook of Conducting Polymers* 2nd edn (New York: Dekker)
[5] Sarathy K V, Narayan K S, Kim J and White J O 2000 Novel fluorescence and morphological structures in gold nanoparticle–polyoctylthiophene based thin films *Chem. Phys. Lett.* **318** 543
[6] Hertel T, Knoesel E, Wolf M and Ertl G 1996 Ultrafast electron dynamics at Cu(111): response of an electron gas to optical excitation *Phys. Rev. Lett.* **76** 535
[7] Ficicoglu F and Kadirgan F 1998 Electrooxidation of ethylene glycol on a platinum doped polyaniline electrode *J. Electroanal. Chem.* **451** 95
[8] Bose C S C and Rajeshwar K 1992 Efficient electrocatalyst assemblies for proton and oxygen reduction: the electrosynthesis and characterization of polypyrrole films containing nanodispersed platinum particles *J. Electroanal. Chem.* **333** 235
[9] Neoh K G, Young T T, Looi N T, Kang E T and Tan K L 1997 Oxidation–reduction interactions between electroactive polymer thin films and Au(III) ions in acid solutions *Chem. Mater.* **9** 2906
[10] Jager E W H, Smela E and Inganas O 2000 Microfabricating conjugated polymer actuators *Science* **290** 540
[11] Bond G C and Thompson D T 1999 Catalysis by gold *Catal. Rev. Sci. Eng.* **41** 319
[12] Kreibig U and Vollmer M 1995 *Optical Properties of Metal Cluster* (Berlin: Springer)
[13] He X and Antonelli D 2002 Recent advances in synthesis and applications of transition metal containing mesoporous molecular sieves *Angew. Chem. Int. Edn* **41** 214
[14] Hepel M 1998 The electrocatalytic oxidation of methanol at finely dispersed platinum nanoparticles in polypyrrole films *J. Electrochem. Soc.* **145** 124
[15] Kao W H and Kuwana T 1984 Electrocatalysis by electrodeposited spherical platinum microparticles dispersed in a polymeric film electrode *J. Am. Chem. Soc.* **106** 473
[16] Kinyanjui J and Hatchett D W 2004 Chemical synthesis of a polyaniline/gold composite using tetrachloroaurate *Chem. Mater.* **16** 3390
[17] Sarma T K and Chattopadhyay A 2004 One pot synthesis of nanoparticles of aqueous colloidal polyaniline and its Au-nanoparticle composite from monomer vapor *J. Phys. Chem.* A **108** 7837
[18] Liu Y-C 2002 New pathway for the autopolymerization of pyrrole on the chlorine- and gold-containing complexes with nanostructures *Langmuir* **18** 9513

[19] Liu Y-C and Chuang T C 2003 Synthesis and characterization of gold/polypyrrole core-shell nanocomposites and elemental gold nanoparticles based on the gold-containing nanocomplexes prepared by electrochemical methods in aqueous solutions *J. Phys. Chem.* B **107** 12383

[20] Selvan S T, Spata J P, Klok H A and Möller M 1998 Gold-polypyrrole core-shell particles in diblock copolymer micelles *Adv. Mater.* **10** 132

[21] Selvan S T, Hayakawa T, Nogami M and Möller M 1999 Block copolymer mediated synthesis of gold quantum dots and novel gold-polypyrrole nanocomposites *J. Phys. Chem.* B **103** 7441

[22] He Y H, Yuan J Y, Shi G Q, Wu P Y and Wang X L 2005 Gold nanoparticle coated polypyrrole nanotubule and its SERS effect *Chem. J. Chin. Univ.* **26** 379

[23] Shin H J, Hwang I-W, Hwang Y-N, Kim D, Han S H, Lee J-S and Cho G 2003 Comparative investigation of energy relaxation dynamics of gold nanoparticles and gold-polypyrrole encapsulated nanoparticles *J. Phys. Chem.* B **107** 4699

[24] Feng L, Li S H, Li Y S, Li H J, Zhang L J, Zhai J, Song Y L, Liu B Q, Jiang L and Zhu D B 2002 Super-hydrophobic surfaces: from natural to artificial *Adv. Mater.* **14** 1857

[25] Yang Y S and Wan M X 2001 Microtubules of polypyrrole synthesized by an electrochemical template-free method *J. Mater. Chem.* **11** 2022

[26] Liu J and Wan M X 2001 Synthesis, characterization and electrical properties of microtubules of polypyrrole synthesized by a template-free method *J. Mater. Chem.* **11** 404

[27] Shen Y Q and Wan M X 1998 In situ doping polymerization of pyrrole with sulfonic acid as a dopant *Synth. Met.* **96** 127

[28] Liu Y, Hwang W, Jian W and Santhanam R 2000 In situ cyclic voltammetry-surface-enhanced Raman spectroscopy: studies on the doping–undoping of polypyrrole film *Thin Solid Film* **374** 85

[29] Warran L F and Anderson D P 1987 Polyrrole films from aqueous electrolytes. The effect of anions upon order *J. Electrochem. Soc.* **134** 101